# Imaging Sphingomyelin- and Cholesterol-Enriched Domains in the Plasma Membrane Using a Novel Probe and Super-Resolution Microscopy

Mitsuhiro Abe and Toshihide Kobayashi

## Abbreviations

| | |
|---|---|
| Chol | cholesterol |
| ELISA | enzyme-linked immunosorbent assay |
| HA | hemagglutinin |
| HILO | highly inclined laminated optical sheet |
| MDCK | *Madin–Darby canine kidney* |
| NA | neuraminidase |
| PALM | photoactivated localization microscopy |
| PH domain | pleckstrin homology domain |
| $PIP_2$ | phosphatidylinositol 4,5-bisphosphate |
| $PIP_3$ | phosphatidylinositol 3,4,5-trisphosphate |
| PLC | phospholipase C |
| PS | phosphatidylserine |
| SIM | structured illumination microscopy |
| SM | sphingomyelin |

M. Abe (✉)
Cellular Informatics Laboratory, RIKEN, Wako, Saitama, Japan
e-mail: abemitsu@riken.jp

T. Kobayashi
Cellular Informatics Laboratory, RIKEN, Wako, Saitama, Japan

UMR 7021 CNRS, Faculté de Pharmacie, Université de Strasbourg, Illkirch, France
e-mail: toshihide.kobayashi@unistra.fr



J. K. Kim et al. (eds.), *Advanced Imaging and Bio Techniques for Convergence Science*, Advances in Experimental Medicine and Biology,
https://doi.org/10.1007/978-981-33-6064-8_4

## Introduction

Lipid rafts are defined as sphingolipid- and sterol-enriched domains (Pike 2006) that form rigid structures in the plasma membrane. The proposed size of the raft is on the order of 10–200 nm (Jacobson et al. 2007; Pike 2006). Lipid rafts are thought to play pivotal roles in membrane trafficking, signal transduction, and the entry of infectious pathogens into cells (Lingwood and Simons 2010; Simons and Toomre 2000). However, the size, function, molecular organization, and dynamics of lipid rafts are not precisely understood for two main reasons.

First, the proposed size of the raft is below the diffraction limit of light (Mizuno et al. 2011). Therefore, conventional fluorescence microscopy is unable to clarify their structure in detail. However, super-resolution optical microscopy systems have recently been developed and provide a resolution beyond the diffraction limit (Toomre and Bewersdorf 2010). These include photoactivated localization microscopy (PALM) (Betzig et al. 2006; Hess et al. 2006), stochastic optical reconstruction microscopy (STORM) (Rust et al. 2006), direct STORM (*d*STORM) (Heilemann et al. 2008; Van De Linde et al. 2011), stimulated emission depletion microscopy (STED) (Willig et al. 2006), structured illumination microscopy (SIM) (Heilemann et al. 2009, 2008), ground-state depletion microscopy followed by individual molecule return (GSDIM) (Folling et al. 2008), blink microscopy (Steinhauer et al. 2008; Vogelsang et al. 2009), and points accumulation for imaging in nanoscale topography (PAINT) (Sharonov and Hochstrasser 2006). Various protein clusters have been revealed with super-resolution microscopy (Hess et al. 2007; Lillemeier et al. 2010; Owen et al. 2010; Schermelleh et al. 2019), and this technique should provide an effective tool for studying lipid rafts in the plasma membrane.

Second, there are no specific probes for lipid rafts (Kraft and Klitzing 2014; Munro 2003). Considerable effort has been made to visualize the lipid components of the rafts in mammalian cells using lipid probes, and both specific lipid-binding proteins (Table 1) and lipid analogs have been widely used as these probes. Cholesterol (Chol) is virtually the exclusive sterol of mammalian cells, which is typically present at 30–40 mol % of plasma membrane lipids. Using the C-terminal domain of perfringolysin O (also referred to as "θ toxin"), which binds the Chol-rich domains in membranes without cytotoxicity (Heuck et al. 2007; Shimada et al. 2002; Verherstraeten et al. 2015), the Chol-rich domains were localized in both the outer and inner leaflets of the mammalian plasma membrane (Abe et al. 2012; Wilhelm et al. 2019). Boron-dipyrromethene (BODIPY)- or polyethylene glycol (PEG)-labeled Chol was developed to monitor the molecular dynamics of sterols in living cells (Hullin-Matsuda et al. 2009; Ikonen and Blom 2016). Sphingomyelin (SM) is one of the major sphingolipids in mammalian cells, which accounts for 10–20 mol% of plasma membrane lipids. To visualize SM in the outer leaflet of the plasma membrane, proteins that specifically bind SM, lysenin, and equinatoxin II were used for the biological analysis of cells (Abe et al. 2012; Bakrac et al. 2010; Kiyokawa et al. 2005). Because lysenin and equinatoxin II preferentially interact with clustered SM-rich domains and dispersed SM-rich domains, respectively, different types of SM domains could be distinguished in the plasma membrane (Makino et al. 2015). The term "clustered SM," used here, indicates small

**Table 1** Nontoxic and protein-based probes for observing lipids at the plasma membrane

| Target lipid | Binding protein |
|---|---|
| Chol | C-terminal domain of perfringolysin O (θ toxin)[b] |
| Clustered SM[a] | Fragment 161–297 amino acid of lysenin[b] |
| Dispersed SM | V8C K69C mutant of equinatoxin II[b] |
| GM1 | B subunit of cholera toxin |
| PS | C2 domain of lactadherin, PH domain of evectin-2 |
| $PIP_2$ | PH domain of PLC-δ[b] |
| $PIP_3$ | PH domain of GRP1, PH domain of Akt |
| SM/Chol complex | Nakanori[b] |

aSmall aggregates of fewer than 10 SM molecules
bPlasmid can be obtained from RIKEN BRC (http://dna.brc.riken.jp/)

aggregates of fewer than 10 SM molecules. ATTO647N-labeled SM was used for the analysis of single molecules in the plasma membrane of living cells (Eggeling et al. 2009). To analyze the ultrastructure of the ganglioside GM1, another sphingolipid in mammalian cells, cholera toxin B, was used for immunoelectron microscopy with sodium dodecyl sulfate (SDS)-treated freeze–fracture replica labeling (SDS-FRL) (Fujita et al. 2007). The distribution of BODIPY–GM1 in the membrane monolayers was examined with a combination of atomic force microscopy and near-field scanning optical microscopy (Coban et al. 2007). The precursors of sphingolipids were also labeled isotopically, and the distribution of sphingolipids in the plasma membrane was mapped with a secondary ion mass spectrometer (Frisz et al. 2013). However, none of these methods detected the complexes of sphingolipid and sterol. Because lipid rafts are defined as complexes of sphingolipid- and sterol-enriched domains (Pike 2006), a protein that specifically binds to complexes of sphingolipid and sterol would be a valuable marker of lipid rafts.

Recently, we identified novel proteins that bind to mixtures of SM and Chol (Bhat et al. 2013; Makino et al. 2017). In extracts from edible mushrooms, we screened for proteins that specifically bind to SM/Chol liposomes. Among them, nakanori was isolated from *Grifola frondosa* and showed strong affinity and specificity for SM/Chol liposomes. Moreover, because nakanori is not cytotoxic to mammalian cells, this protein should be a reliable marker of SM/Chol domains in living cells. Here, we describe a method of visualizing SM- and Chol-rich membrane domains with a combination of nakanori and super-resolution microscopy.

## A Novel Protein, Nakanori Strongly Binds SM/Chol Mixtures

In the proteins extracted from the edible mushroom *G. frondosa* (Fig. 1a), we screened for those that specifically bound to liposomes containing equimolar SM

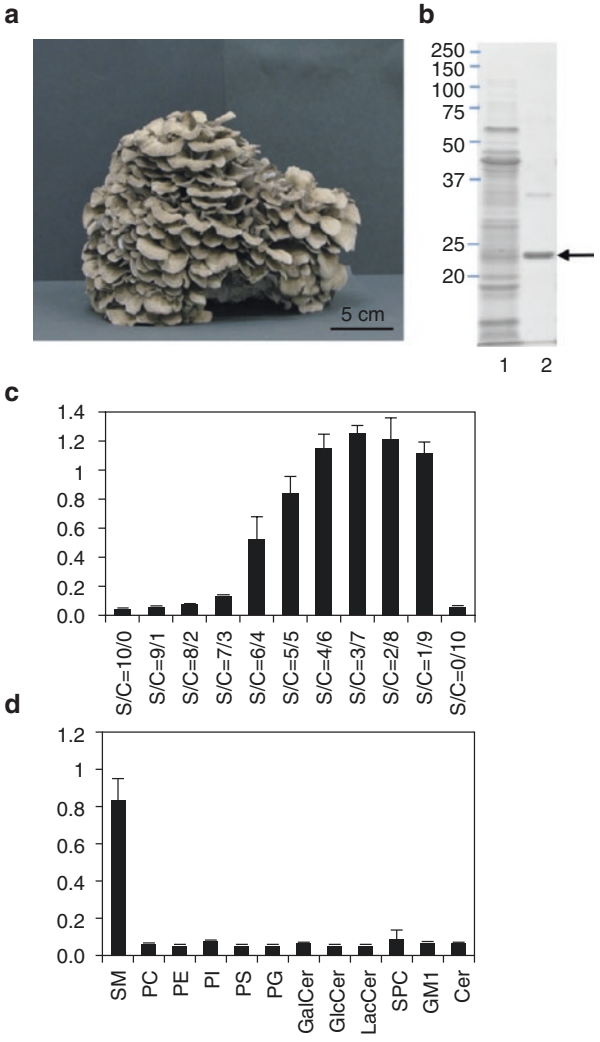


**Fig. 1** Isolation and characterization of SM/Chol-binding protein, nakanori, from mushroom *Grifola frondosa*. (**a**) Mushroom *Grifola frondosa.* Scale bar = 5 cm. (**b**) Screening of SM/Chol-binding protein from *G. frondosa*. The supernatant (lane 1) and pellet (lane 2) fractions after incubation of 11,000 rpm supernatant of *G. frondosa* extract with SM/Chol liposomes. Arrow indicates the position of nakanori. (**c**) Binding of purified nakanori to liposomes composed of different SM(S)/Chol(C) ratios by ELISA. (**d**) Binding of nakanori to indicated lipids in the presence of equimolar Chol by ELISA. Data are mean of triplicate experiments ± SD. *SM* porcine brain sphingomyelin, *PC* egg phosphatidylcholine, *PE* 1-palmitoyl-2-oleoyl-*sn*-glycero-3-phosphoethanolamine, *PS* porcine brain phosphatidylserine, *PI* bovine liver phosphatidylinositol, *PG* 1,2-dioleoyl-*sn*-glycero-3-phospho-(1′-*rac*-glycerol), *GalCer* porcine brain cerebroside, *GlcCer* human glucosylceramide, *LacCer* lactosylceramide, *SPC* sphingosylphosphorylcholine, *GM1* bovine brain ganglioside GM1, *Cer* porcine brain ceramide. Adapted from reference (Makino et al. 2017)

and Chol. After incubation with SM/Chol liposomes, several proteins were identified as SM/Chol-binding proteins. A mass spectrometric analysis and molecular cloning determined the sequence of the major protein (arrow in Fig. 1b), showing that it contains 202 amino acid residues, with no obvious consensus motifs. We designated this protein "nakanori," derived from the Japanese for "mid-raft rider." After the recombinant nakanori protein was purified from *Escherichia coli*, its binding specificity for several lipids was examined with enzyme-linked immunosorbent assays (ELISAs) (Fig. 1c and d). Nakanori bound neither SM alone nor Chol alone but significantly bound a mixture of SM and Chol (Fig. 1c). The ELISA also revealed that nakanori interacts with the SM/Chol complex but not with the other lipid/Chol mixtures (Fig. 1d), indicating its high specificity for SM/Chol mixtures. The affinity ($K_d$) of nakanori for equimolar SM/Chol membranes was determined. Measurement with a quartz crystal microbalance revealed a $K_d$ value of 141 ± 4 nM (Makino et al. 2017).

## SIM Analysis Suggesting That Influenza Virus Buds from the Rim of the SM/Chol Domain

It has been proposed that the influenza virus buds from cells at sites around the lipid rafts, where the viral proteins, hemagglutinin (HA) and neuraminidase (NA) assemble (Gerl et al. 2012; Scheiffele et al. 1999). To observe the budding of the influenza virus from the plasma membranes of mammalian cells, *Madin–Darby canine kidney* (MDCK) cells were infected with the virus for 24 h in the presence of a NA inhibitor. Nakanori was fused with the fluorescent protein mKate, and the fusion protein (mKate–nakanori) was expressed in *E. coli* and purified (Makino et al. 2017). The specificity of mKate–nakanori for SM was confirmed with a biochemical assay. After mKate–nakanori was bound to the SM- and Chol-rich complexes in living MDCK cells, the protein interacting with SM/Chol was chemically fixed. The cells were then stained with an anti-influenza A H1N1 antibody, and SM/Chol and the influenza virus were observed at the plasma membrane with confocal microscopy (Fig. 2a). Although distributions of SM/Chol and the influenza virus were detected in the plasma membrane, their detailed structures and co-localization were far from obvious because of the diffraction limit of light. To clarify them, we observed the patterns with super-resolution microscopy. Structured illumination microscopy (SIM) images indicated that the virus budded from the rim of the SM/Chol domain (Fig. 2b). Here, we use the term "SM/Chol domain" to indicate the specific area of the membrane where the labeling density of nakanori is high. Several lines of evidence suggest that the influenza viral proteins, HA and NA, associate with lipid rafts, whereas the viral M2 protein does not (Blom et al. 2001; Gerl et al. 2012; Zhang et al. 2000). Taken together, these data imply that associations of raft- and non-raft proteins form at the rim of the SM/Chol domain, followed by the budding and fission of the influenza virus.

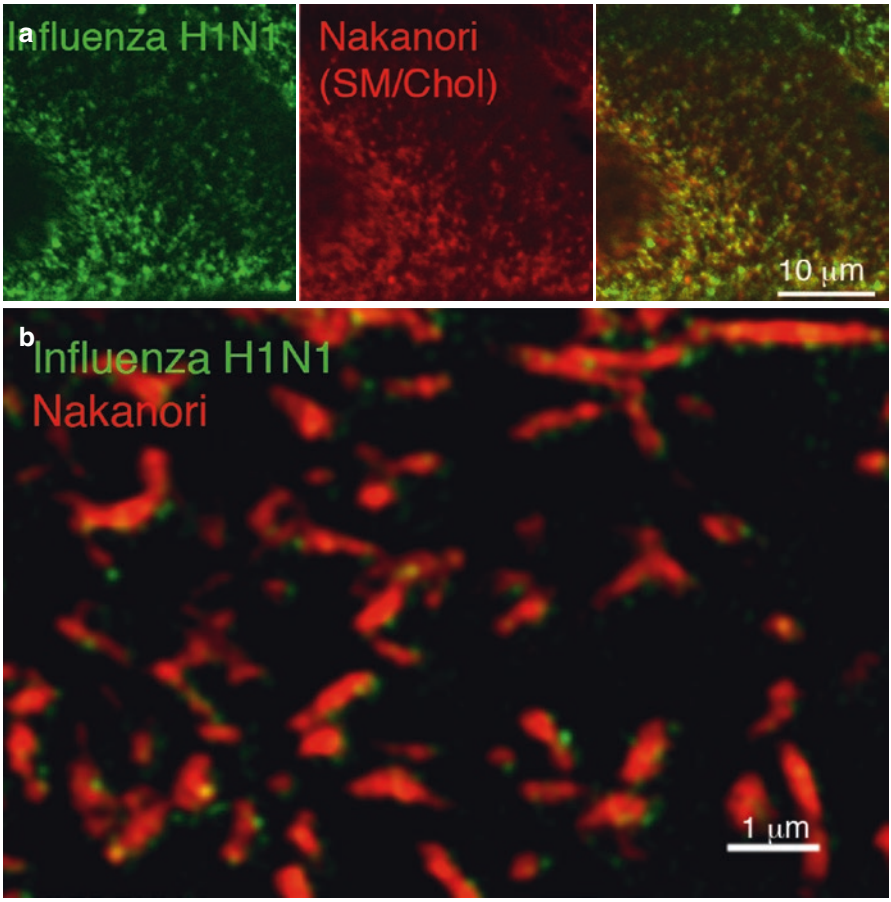


**Fig. 2** Images of SM/Chol domains and influenza virus in the apical plasma membrane in MDCK cells. MDCK cells were incubated for 24 h in the presence of NA inhibitor after infection with influenza virus. Cells were then labeled with mKate–nakanori (red) and anti-influenza A H1N1 antibody (MAB8256; EMD–Millipore) (green). (**a**) Confocal images. Scale bar = 10 μm. (**b**) SIM images. Images were obtained at the apical face of the plasma membrane. Scale bar = 1 μm. Adapted from reference (Makino et al. 2017)

## PALM Analysis Indicating the Transbilayer Co-localization Between SM/Chol Domains and $PIP_2$ Domains

We tried to observe the SM/Chol domains in the apical plasma membrane using another super-resolution microscopy, PALM. For this purpose, nakanori was fused with the photoswitchable fluorescent protein PAmCherry1 (Subach et al. 2009), and the recombinant protein (PAmCherry–nakanori) was purified from *E. coli* (Makino et al. 2017). Because total internal reflection fluorescence (TIRF) illumination

restricts the excitation region to a few hundred nanometers above the glass, it is unsuitable for observing structures in the apical membrane. Therefore, we used instead highly inclined laminated optical sheet (HILO) illumination (Tokunaga et al. 2008), which excites a higher region above the glass with low background. The SM- and Chol-rich domains stained with PAmCherry–nakanori were observed in the apical membrane with a PALM analysis with HILO illumination (Fig. 3). The SM/Chol in the outer leaflet was visualized with PALM after it was labeled with exogenous PAmCherry–nakanori (Fig. 3, red). Small domains of SM/Chol were observed at the apical plasma membrane.

Several analyses have suggested that phosphatidylinositol 4,5-bisphosphate ($PIP_2$) associates with the lipid raft fraction of membranes (Brown and London 1998; Hope and Pike 1996; Laux et al. 2000). $PIP_2$ occurs in the inner leaflet in mammalian cells, whereas the SM/Chol complex is enriched in the outer leaflet of the plasma membrane (Fujita et al. 2009; Murate et al. 2015). To address the possibility that $PIP_2$ forms domains in the inner leaflet just below the SM/Chol domains, we examined the localization of SM/Chol and $PIP_2$ simultaneously (Fig. 3) (Makino et al. 2017). To observe $PIP_2$ in the inner leaflet with PALM, pleckstrin homology (PH) domain of phospholipase C δ (PLC-δ) was fused with the photoswitchable fluorescent protein Dronpa (Ando et al. 2004), and the fusion protein (Dronpa–PLC-δPH) was expressed in LLC-PK1 cells (Fig. 3, green). Small colocalized domains of PAmCherry–nakanori and Dronpa–PLC-δPH were observed at the apical plasma membrane (Fig. 3). These results indicate that $PIP_2$ forms domains in the inner leaflet, just below the SM/Chol domains in the outer leaflet.

There are several possible explanations of why the $PIP_2$ domains form just beneath the SM/Chol domains. First, SM/Chol and $PIP_2$ may interact, directly or

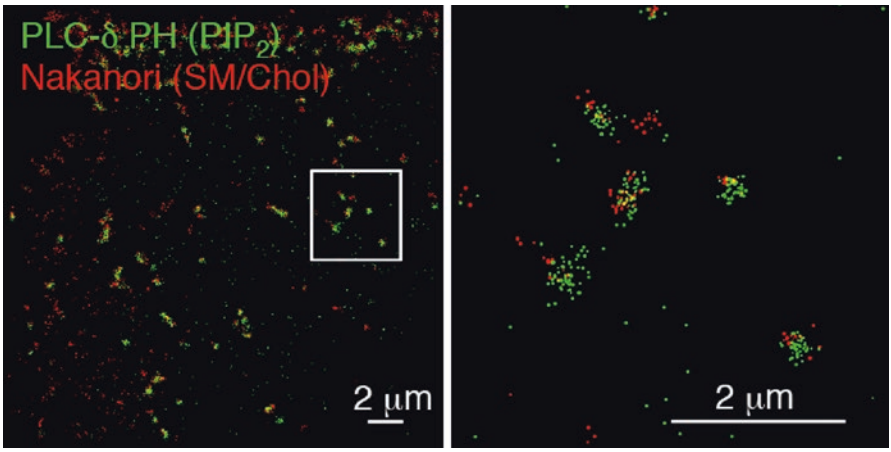


**Fig. 3** Transbilayer co-localization between the SM-rich domains on the outer leaflet and $PIP_2$-rich domains on the inner leaflet of the plasma membrane. LLC-PK1 cells expressing Dronpa–PLC-δPH (green) were stained with PAmCherry–nakanori (red). Bars, 2 μm. Adapted from reference (Makino et al. 2017)

indirectly. Indeed, it has been shown that long-acyl-chain lipids in both leaflets stabilize cholesterol-dependent transbilayer interactions (Raghupathy et al. 2015). Second, the production of $PIP_2$ may be restricted to just below the SM/Chol domains. We have shown that the kinase required for the production of $PIP_2$ is enriched in the inner leaflet, on the opposite side to the clustered SM domains (Abe et al. 2012). Therefore, if this is the case, why the mobility of $PIP_2$ is restricted to around the SM/Chol domains must be explained. Further experiments are required to understand the molecular mechanisms underlying the transbilayer co-localization between SM/Chol domains and $PIP_2$ domains.

**Acknowledgments** I thank Toshiyuki Watanabe and Carl Zeiss Microscopy Co. Ltd. Japan for SIM images, and Hideaki Mizuno for PALM images. We are grateful to Asami Makino and Takehiko Inaba for biochemical analysis of nakanori. The original work was supported by the Lipid Dynamics Program of RIKEN, and the Grant-in-Aid from the Ministry of Education, Culture, Sports, Science, and Technology of Japan (22390018, 25293015) and Naito Foundation.

## References

Abe M, Makino A, Hullin-Matsuda F et al (2012) A role for sphingomyelin-rich lipid domains in the accumulation of phosphatidylinositol-4,5-bisphosphate to the cleavage furrow during cytokinesis. Mol Cell Biol 32:1396–1407

Ando R, Mizuno H, Miyawaki A (2004) Regulated fast nucleocytoplasmic shuttling observed by reversible protein highlighting. Science 306:1370–1373

Bakrac B, Kladnik A, Macek P et al (2010) A toxin-based probe reveals cytoplasmic exposure of Golgi sphingomyelin. J Biol Chem 285:22186–22195

Betzig E, Patterson GH, Sougrat R et al (2006) Imaging intracellular fluorescent proteins at nanometer resolution. Science 313:1642–1645

Bhat HB, Kishimoto T, Abe M et al (2013) Binding of a pleurotolysin ortholog from Pleurotus eryngii to sphingomyelin and cholesterol-rich membrane domains. J Lipid Res 54:2933–2943

Blom TS, Koivusalo M, Kuismanen E et al (2001) Mass spectrometric analysis reveals an increase in plasma membrane polyunsaturated phospholipid species upon cellular cholesterol loading. Biochemistry 40:14635–14644

Brown DA, London E (1998) Functions of lipid rafts in biological membranes. Annu Rev Cell Dev Biol 14:111–136

Coban O, Burger M, Laliberte M et al (2007) Ganglioside partitioning and aggregation in phase-separated monolayers characterized by bodipy GM1 monomer/dimer emission. Langmuir 23:6704–6711

Eggeling C, Ringemann C, Medda R et al (2009) Direct observation of the nanoscale dynamics of membrane lipids in a living cell. Nature 457:1159–1162

Folling J, Bossi M, Bock H et al (2008) Fluorescence nanoscopy by ground-state depletion and single-molecule return. Nat Methods 5:943–945

Frisz JF, Lou K, Klitzing HA et al (2013) Direct chemical evidence for sphingolipid domains in the plasma membranes of fibroblasts. Proc Natl Acad Sci USA 110:E613–E622

Fujita A, Cheng J, Hirakawa M et al (2007) Gangliosides GM1 and GM3 in the living cell membrane form clusters susceptible to cholesterol depletion and chilling. Mol Biol Cell 18:2112–2122

Fujita A, Cheng J, Tauchi-Sato K et al (2009) A distinct pool of phosphatidylinositol 4,5-bisphosphate in caveolae revealed by a nanoscale labeling technique. Proc Natl Acad Sci USA 106:9256–9261

Gerl MJ, Sampaio JL, Urban S et al (2012) Quantitative analysis of the lipidomes of the influenza virus envelope and MDCK cell apical membrane. J Cell Biol 196:213–221
Heilemann M, Van De Linde S, Schuttpelz M et al (2008) Subdiffraction-resolution fluorescence imaging with conventional fluorescent probes. Angew Chem Int Ed Engl 47:6172–6176
Heilemann M, Van De Linde S, Mukherjee A et al (2009) Super-resolution imaging with small organic fluorophores. Angew Chem Int Ed Engl 48:6903–6908
Hess ST, Girirajan TP, Mason MD (2006) Ultra-high resolution imaging by fluorescence photoactivation localization microscopy. Biophys J 91:4258–4272
Hess ST, Gould TJ, Gudheti MV et al (2007) Dynamic clustered distribution of hemagglutinin resolved at 40 nm in living cell membranes discriminates between raft theories. Proc Natl Acad Sci USA 104:17370–17375
Heuck AP, Savva CG, Holzenburg A et al (2007) Conformational changes that effect oligomerization and initiate pore formation are triggered throughout perfringolysin O upon binding to cholesterol. J Biol Chem 282:22629–22637
Hope HR, Pike LJ (1996) Phosphoinositides and phosphoinositide-utilizing enzymes in detergent-insoluble lipid domains. Mol Biol Cell 7:843–851
Hullin-Matsuda F, Ishitsuka R, Takahashi M et al (2009) Imaging lipid membrane domains with lipid-specific probes. Methods Mol Biol 580:203–220
Ikonen E, Blom T (2016) Lipoprotein-mediated delivery of BODIPY-labeled sterol and sphingolipid analogs reveals lipid transport mechanisms in mammalian cells. Chem Phys Lipids 194:29–36
Jacobson K, Mouritsen OG, Anderson RG (2007) Lipid rafts: at a crossroad between cell biology and physics. Nat Cell Biol 9:7–14
Kiyokawa E, Baba T, Otsuka N et al (2005) Spatial and functional heterogeneity of sphingolipid-rich membrane domains. J Biol Chem 280:24072–24084
Kraft ML, Klitzing HA (2014) Imaging lipids with secondary ion mass spectrometry. Biochim Biophys Acta 1841:1108–1119
Laux T, Fukami K, Thelen M et al (2000) GAP43, MARCKS, and CAP23 modulate PI(4,5)P(2) at plasmalemmal rafts, and regulate cell cortex actin dynamics through a common mechanism. J Cell Biol 149:1455–1472
Lillemeier BF, Mortelmaier MA, Forstner MB et al (2010) TCR and Lat are expressed on separate protein islands on T cell membranes and concatenate during activation. Nat Immunol 11:90–96
Lingwood D, Simons K (2010) Lipid rafts as a membrane-organizing principle. Science 327:46–50
Makino A, Abe M, Murate M et al (2015) Visualization of the heterogeneous membrane distribution of sphingomyelin associated with cytokinesis, cell polarity, and sphingolipidosis. FASEB J 29:477–493
Makino A, Abe M, Ishitsuka R et al (2017) A novel sphingomyelin/cholesterol domain-specific probe reveals the dynamics of the membrane domains during virus release and in Niemann-Pick type C. FASEB J 31:1301–1322
Mizuno H, Abe M, Dedecker P et al (2011) Fluorescent probes for superresolution imaging of lipid domains on the plasma membrane. Chem Sci 2:1548–1553
Munro S (2003) Lipid rafts: elusive or illusive? Cell 115:377–388
Murate M, Abe M, Kasahara K et al (2015) Transbilayer distribution of lipids at nano scale. J Cell Sci 128:1627–1638
Owen DM, Rentero C, Rossy J et al (2010) PALM imaging and cluster analysis of protein heterogeneity at the cell surface. J Biophotonics 3:446–454
Pike LJ (2006) Rafts defined: a report on the keystone symposium on lipid rafts and cell function. J Lipid Res 47:1597–1598
Raghupathy R, Anilkumar AA, Polley A et al (2015) Transbilayer lipid interactions mediate nanoclustering of lipid-anchored proteins. Cell 161:581–594
Rust MJ, Bates M, Zhuang X (2006) Sub-diffraction-limit imaging by stochastic optical reconstruction microscopy (STORM). Nat Methods 3:793–795
Scheiffele P, Rietveld A, Wilk T et al (1999) Influenza viruses select ordered lipid domains during budding from the plasma membrane. J Biol Chem 274:2038–2044

Schermelleh L, Ferrand A, Huser T et al (2019) Super-resolution microscopy demystified. Nat Cell Biol 21:72–84

Sharonov A, Hochstrasser RM (2006) Wide-field subdiffraction imaging by accumulated binding of diffusing probes. Proc Natl Acad Sci USA 103:18911–18916

Shimada Y, Maruya M, Iwashita S et al (2002) The C-terminal domain of perfringolysin O is an essential cholesterol-binding unit targeting to cholesterol-rich microdomains. Eur J Biochem 269:6195–6203

Simons K, Toomre D (2000) Lipid rafts and signal transduction. Nat Rev Mol Cell Biol 1:31–39

Steinhauer C, Forthmann C, Vogelsang J et al (2008) Superresolution microscopy on the basis of engineered dark states. J Am Chem Soc 130:16840–16841

Subach FV, Patterson GH, Manley S et al (2009) Photoactivatable mCherry for high-resolution two-color fluorescence microscopy. Nat Methods 6:153–159

Tokunaga M, Imamoto N, Sakata-Sogawa K (2008) Highly inclined thin illumination enables clear single-molecule imaging in cells. Nat Methods 5:159–161

Toomre D, Bewersdorf J (2010) A new wave of cellular imaging. Annu Rev Cell Dev Biol 26:285–314

Van De Linde S, Loschberger A, Klein T et al (2011) Direct stochastic optical reconstruction microscopy with standard fluorescent probes. Nat Protoc 6:991–1009

Verherstraeten S, Goossens E, Valgaeren B et al (2015) Perfringolysin O: the underrated *Clostridium perfringens* toxin? Toxins (Basel) 7:1702–1721

Vogelsang J, Cordes T, Forthmann C et al (2009) Controlling the fluorescence of ordinary oxazine dyes for single-molecule switching and superresolution microscopy. Proc Natl Acad Sci USA 106:8107–8112

Wilhelm LP, Voilquin L, Kobayashi T et al (2019) Intracellular and plasma membrane cholesterol labeling and quantification using filipin and GFP-D4. Methods Mol Biol 1949:137–152

Willig KI, Kellner RR, Medda R et al (2006) Nanoscale resolution in GFP-based microscopy. Nat Methods 3:721–723

Zhang J, Pekosz A, Lamb RA (2000) Influenza virus assembly and lipid raft microdomains: a role for the cytoplasmic tails of the spike glycoproteins. J Virol 74:4634–4644